

# The CYPome of *Sorangium cellulosum* So ce56 and Identification of CYP109D1 as a New Fatty Acid Hydroxylase

Yogan Khatri,<sup>1</sup> Frank Hannemann,<sup>1</sup> Kerstin M. Ewen,<sup>1</sup> Dominik Pistorius,<sup>2</sup> Olena Perlova,<sup>2</sup> Norio Kagawa,<sup>3</sup> Alexander O. Brachmann,<sup>2</sup> Rolf Müller,<sup>2</sup> and Rita Bernhardt<sup>1,\*</sup>

<sup>1</sup>Department of Biochemistry, Saarland University, Campus B2.2, 66123 Saarbrücken, Germany

<sup>2</sup>Helmholtz Institute for Pharmaceutical Research Saarland, Helmholtz Centre for Infection Research and Department of Pharmaceutical Biotechnology, Saarland University, D-66041 Saarbrücken, Germany

<sup>3</sup>Global COE program, Nagoya University of Graduate School of Medicine, Showaku, Nagoya, Japan

\*Correspondence: ritabern@mx.uni-saarland.de

DOI 10.1016/j.chembiol.2010.10.010

## SUMMARY

The first systematic study of the complete cytochrome P450 complement (CYPome) of *Sorangium cellulosum* So ce56, which is a producer of important secondary metabolites and has the largest bacterial genome sequenced to date, is presented. We describe the bioinformatic analysis of the So ce56 cytochrome P450 complement consisting of 21 putative P450 genes. Because fatty acids play a pivotal role during the complex life cycle of myxobacteria, we focused our studies on the characterization of fatty acid hydroxylases. Three novel potential fatty acid hydroxylases (CYP109D1, CYP264A1, and CYP266A1) were used for detailed characterization. One of them, CYP109D1 was able to perform subterminal hydroxylation of saturated fatty acids with the support of two autologous and one heterologous electron transfer system(s). The kinetic parameters for the product hydroxylation were derived.

## INTRODUCTION

Cytochrome P450-dependent monooxygenase systems are found throughout the biological kingdoms from bacteria to mammals. Enzymes of the cytochrome P450 superfamily play a critical role during the bioactivation and detoxification of a wide variety of drugs and xenobiotics, and in the biosynthesis of endogenous compounds and secondary metabolites (Bernhardt, 1996, 2006; Graziani et al., 1998; Zhao et al., 2008; Buntin et al., 2008).

Due to the results of various genome projects, sequence information for P450s has increased in recent years. Unfortunately, the functional studies of the corresponding P450s are lagging far behind. Very recently, the genome sequence project of the myxobacterium *Sorangium cellulosum* So ce56 has disclosed 21 open reading frames (ORFs) of P450s (Schneiker et al., 2007). The genus *Sorangium* is regarded as the most promising resource for novel natural products and ~46% of all known myxobacterial compounds are derived from this genus (Gerth et al.,

2003) including novel antimicrobial macrolides (Wenzel and Müller, 2009), and a novel class of antineoplastic agents: the epothilones and their analogs (Mulzer, 2008). Moreover, members of the myxobacteria have unique features like gliding motility, and forming “social” multicellular hunting and feeding swarms (Whilworth, 2007). It has been shown that several fatty acids and lipids derived from them play a central role during these complex physiological processes (Ring et al., 2009; Curtis et al., 2006). The fatty acid profiles in myxobacteria are very complex and up to 40 different compounds belonging to all known classes of fatty acids have been detected (Ware and Dworkin, 1973; Bode et al., 2005). It was also shown that odd numbered, iso- or anteiso-branched fatty acids are predominant in myxobacteria and some other gliding bacteria (Kaneda, 1991). Furthermore, the unexpected abundance of fatty acids has been demonstrated to play a vital role during fruiting body formation in myxobacteria (Ring et al., 2009; Kaiser, 2003; Bode et al., 2006). Thus, the presence of a relatively high number of P450s in *Sorangium cellulosum* So ce56 could be due to their involvement in important physiological functions during its complex life cycle and also to the ability of this bacterium to produce novel secondary metabolites.

In this study, the bioinformatic analysis of the cytochrome P450 complement (CYPome) of *S. cellulosum* So ce56 is described for the very first time. As several terminal and subterminal hydroxylations of fatty acids are generally ascribed to the action of cytochromes P450 (Green et al., 2001; Chun et al., 2007), potential fatty acid hydroxylating P450s in So ce56 were identified and characterized.

## RESULTS

### Bioinformatic Analysis

*Sorangium cellulosum* So ce56 has the largest bacterial genome sequenced to date, which revealed the presence of 21 putative cytochromes P450 (Schneiker et al., 2007). The distribution of P450s is shown in a physical map of the 13.1 Mb genome (Figure 1). The genomic abundance of P450 comprises 0.15% of all coding sequences, which is relatively low compared with 0.2% and 0.4% as described for *Streptomyces coelicolor* A(3)2 and *Streptomyces avermitilis*, respectively (Lamb et al., 2003).

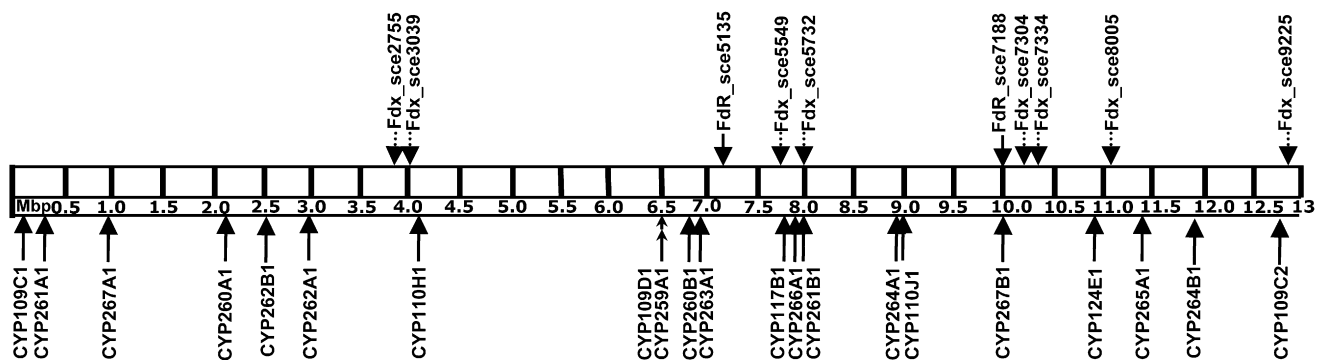


**Figure 1. Physical Map of the *Sorangium cellulosum* So ce56 Chromosome and Distribution of Cytochrome P450, Ferredoxin (Fdx), and Ferredoxin Reductase (Fdr) Genes**

All 21 So ce56 P450s with respective P450 annotation are assigned in their genomic location of the 13,033,779 base pairs genome. The distribution of Fdx and Fdr is represented with respect to the gene number as annotated in NCBI.

The conserved P450 structural core is formed by a four-helix bundle comprised with three parallel helices (D, L, and I) and one antiparallel helix E where the prosthetic heme group is confined between the distal I-helix and proximal L-helix and bound to the adjacent “cys” of heme-domains (Presnell and Cohen, 1989; Dawson et al., 1976). In this study, all 21 P450s of *S. cellulosum* So ce56 possess a conserved I-helix that contains the signature amino acid sequence (A/G)Gx(E/D)T. The highly conserved threonine is believed to be involved in

catlysis (Martinis et al., 1989; Vidakovic et al., 1998). Similarly, a glutamic acid and an arginine in the EXXR motif of the K-helix are also conserved in all the P450s of So ce56. Both of these residues help to form a set of salt-bridge interactions that participate in the formation of the final P450 tertiary structure (Hasemann et al., 1995). Moreover, the heme-binding signature amino acid sequence FxxGx(H/R)xCxG is absolutely conserved in 19 of the 21 P450s (Table 1). The absolutely conserved cysteine, which forms two hydrogen bonds with the neighboring back-bone

**Table 1. Conserved Domains of the *Sorangium cellulosum* So ce56 CYPome**

P450s of So ce56 <sup>a</sup>	So ce56 Gene Name <sup>b</sup>	I-Helix	K-Helix	Heme Binding Domain
CYP109C1	sce0122	226AGTETA <sup>231</sup>	264EEVLR <sup>268</sup>	329 <b>FGHGIHFCIG</b> <sup>338</sup>
CYP109C2	sce8913	226AGHETT <sup>231</sup>	264EEVLR <sup>288</sup>	329 <b>FGHGIHFCIG</b> <sup>338</sup>
CYP109D1	sce4633	241AGNDTT <sup>246</sup>	279EETLR <sup>283</sup>	344 <b>FGQGTTHFCIG</b> <sup>353</sup>
CYP110H1	sce3065	251AGHETT <sup>256</sup>	304KEALR <sup>308</sup>	375 <b>FGGGHRRICIG</b> <sup>384</sup>
CYP110J1	sce6424	255AGHETT <sup>260</sup>	308LEALR <sup>312</sup>	379 <b>FGGGARRCLG</b> <sup>388</sup>
CYP117B1	sce5528	272AGHETS <sup>277</sup>	326REALR <sup>330</sup>	399 <b>FGGGAHFCLG</b> <sup>408</sup>
CYP124E1	sce7867	239AGHDTT <sup>244</sup>	277EEMLR <sup>281</sup>	342 <b>FGIGPHVCLG</b> <sup>351</sup>
CYP259A1	sce4635	250AGHETS <sup>255</sup>	306REVLR <sup>310</sup>	379 <b>FGGGPHFCIG</b> <sup>388</sup>
CYP260A1	sce1588	279GGYETT <sup>284</sup>	317EEGMR <sup>321</sup>	331 <b>FGGGAHFCVCG</b> <sup>340</sup>
CYP260B1	sce4806	228GSYETT <sup>233</sup>	266EESTR <sup>270</sup>	331 <b>FGGGLHYCVG</b> <sup>340</sup>
CYP261A1	sce0200	287AGEDTT <sup>292</sup>	344QETLR <sup>348</sup>	421 <b>FGSGPRVCPG</b> <sup>430</sup>
CYP261B1	sce5725	299AGEDTT <sup>304</sup>	355QETLR <sup>359</sup>	431 <b>FGGGPRVCPG</b> <sup>440</sup>
CYP262A1	sce2191	247AGNETT <sup>252</sup>	302QEAMR <sup>306</sup>	376 <b>FGGGPRQCIG</b> <sup>385</sup>
CYP262B1	sce1860	279AGYETT <sup>284</sup>	334QEALR <sup>338</sup>	408 <b>FGIGQRQCVG</b> <sup>417</sup>
CYP263A1	sce4885	263VGHETS <sup>268</sup>	318NECLR <sup>322</sup>	392 <b>FGAGQRICLG</b> <sup>401</sup>
CYP264A1	sce6323	229GGLETT <sup>234</sup>	267EEMMR <sup>271</sup>	331 <b>FGHGAHFCLG</b> <sup>340</sup>
CYP264B1	sce8551	235AGLETS <sup>240</sup>	273EEVMR <sup>277</sup>	338 <b>FGHGAHFCLG</b> <sup>347</sup>
CYP265A1	sce8224	234GGLDTT <sup>239</sup>	272EEILR <sup>276</sup>	337 <b>LGAGPHHCLG</b> <sup>346</sup>
CYP266A1	sce5624	249AGFETV <sup>254</sup>	287DEMLR <sup>291</sup>	353 <b>FGGGHHFCIG</b> <sup>362</sup>
CYP267A1	sce0675	263GGHETT <sup>268</sup>	301EELLR <sup>305</sup>	366 <b>LGLGVHYCAG</b> <sup>375</sup>
CYP267B1	sce7167	243AGHETT <sup>248</sup>	281EEALR <sup>285</sup>	347 <b>FGGGIHFCLG</b> <sup>356</sup>

Residues conserved in the I-helix (T), the K-helix (E and R), and the heme-binding motif (F, G, and C) are highlighted in bold. The presence of amino acid leucine (L) in the heme-binding domain of CYP265A1 and CYP267A1, instead of the usually conserved phenylalanine (F) residue, is depicted in italics. The numbers shown at the beginning and the end of each domain represent the relevant position of the amino acid.

<sup>a</sup> CYP names as annotated at <http://drnelson.utmem.edu/CytochromeP450.html>.

<sup>b</sup> Gene names as annotated in National Center for Biotechnology Information.

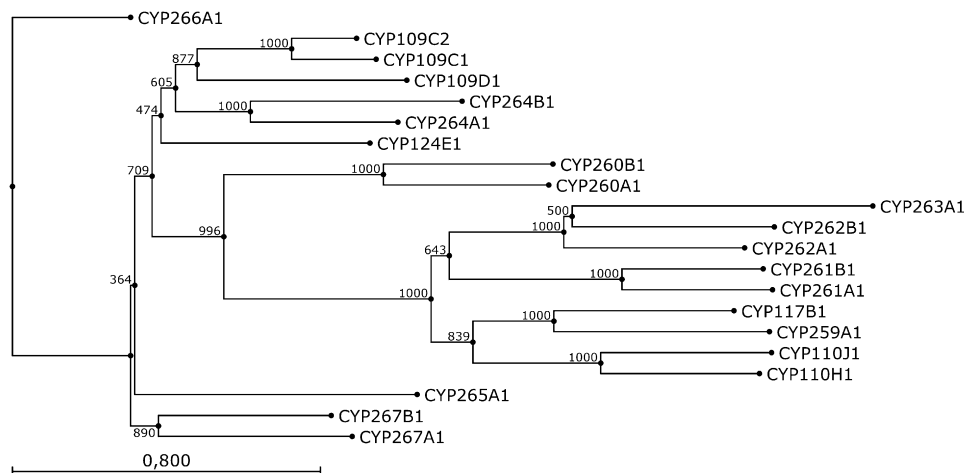


**Figure 2. Phylogenetic Tree of *Sorangium cellulosum* So ce56 Cytochromes P450**

The alignment was done with 10 gap setting and 1 gap extension having slow (very accurate) alignment input in the CLC Workbench. The tree was constructed by using the Neighbor Joining Algorithm with performing boot strap analysis of 1000 times replicate. Bootstrap values are shown at branch nodes. The bar in the left corner indicates 0.8 amino acid substitutions per amino acid for the branch length.

amide, is the proximal or “fifth” ligand to the heme iron. The sulfur ligand is a thiolate causing the 450 nm Soret absorbance observed for the ferrous-CO complex (Dawson et al., 1976) that is the origin of the characteristic name of the P450s. However, in two of the P450s, CYP265A1 and CYP267A1, the aromatic amino acid phenylalanine (F) is replaced by the neutral aliphatic amino acid leucine (L). Though the mutation of F293 in P450-BM3 (CYP102) to histidine (H) has shown a pronounced effect on the reduction potential (Ost et al., 2001) of this enzyme, a detailed study of this heme variant has not been performed so far. In fact, structure was solved, and detailed characterization was done—including demonstrating that the oxy complex was stabilized and that the Fe<sup>II</sup>-CO complex Soret was blue shifted. The implication is that the thiolate bond is severely affected once the Phe is mutated, and thus that its role is in heme potential poise to enable oxygen reduction and activation.

We have identified nine novel P450 families represented by 14 of the 21 P450s from So ce56: CYP259 (CYP259A1), CYP260 (CYP260A1 and CYP260B1), CYP261 (CYP261A1 and CYP261B1), CYP262 (CYP262A1 and CYP262B1), CYP263 (CYP263A1), CYP264 (CYP264A1 and CYP264B1), CYP265 (CYP265A1), CYP266 (CYP266A1), and CYP267 (CYP267A1 and CYP267B1). The other seven P450s were members of known P450 families. Three of them, CYP109C1, CYP109C2, and CYP109D1, are members of the CYP109 family. It has been shown that CYP109B1 from *Bacillus subtilis* is able to bind and oxidize a broad range of substrates including fatty acids, primary n-alcohols and terpenoids (Girhard et al., 2010). Two of the P450s (CYP110H1 and CYP110J1) belong to the CYP110 family. It was shown that CYP110 from *Anabaena* 7120 is able to bind long-chain saturated and unsaturated fatty acids (Torres et al., 2005). Moreover, CYP117B1 and CYP124E1 are members of the assigned families CYP117 and CYP124, respectively. A CYP117 related gene was also shown to be present in *Bradyrhizobium japonicum* but the biochemical function of the gene product was uncertain (Tully et al., 1998).

However, very recently it was shown that CYP124 from *Mycobacterium tuberculosis* performed the preferential oxidation of methyl-branched lipids (Johnston et al., 2009). Moreover, the relatedness of *S. cellulosum* So ce56 P450s among each other was also studied and a phylogenetic tree was constructed (Figure 2). CYP266A1 was found to be distantly related to other P450s of So ce56.

#### Search for Potential Fatty Acid Hydroxylating P450s in So ce56

The important role of lipids during the complex life cycle of myxobacteria (Ring et al., 2009; Bode et al., 2006) guided us to presume fatty acids as potential substrates for some of the P450s. The amino acid sequences of well known fatty acid hydroxylating P450s, CYP102A1 from *Bacillus megaterium* (Shirane et al., 1993; Davis et al., 1996), CYP102A2 and CYP102A3 from *B. subtilis* (Gustafsson et al., 2004), P450foxy from *Fusarium oxysporum* (Kitazume et al., 2002), CYP152A2 from *Clostridium acetobutylicum* (Girhard et al., 2007), P450Biol from *B. subtilis* (Green et al., 2001), and CYP105D5 from *S. coelicolor* A(3)2 (Chun et al., 2007) were retrieved from EMBL. The amino acid sequences of P450s from So ce56 were aligned with those fatty acid hydroxylases and an unrooted phylogenetic tree was constructed (see Figure S1 available online). It was found that 10 of the P450s, CYP109 (CYP109C1, CYP109C2 and CYP109D1), CYP124E1, CYP264 (CYP264A1 and CYP264B1), CYP265A1, CYP266A1, and CYP267 (CYP267A1 and CYP267B1) from So ce56 were clustered with P450Biol from *B. subtilis* and CYP105D5 from *S. coelicolor* A(3)2.

Among the 10 putative fatty acid hydroxylating P450s, the three P450s (CYP109D1, CYP264A1, and CYP266A1) showing the highest sequence homology to the two well characterized fatty acid hydroxylases (P450Biol and CYP105D5) were chosen for further studies (data not shown). Moreover, CYP109D1 is a member of the assigned CYP109 family, whereas CYP264A1 and CYP266A1 represent members of the novel CYP264 and CYP266 families.

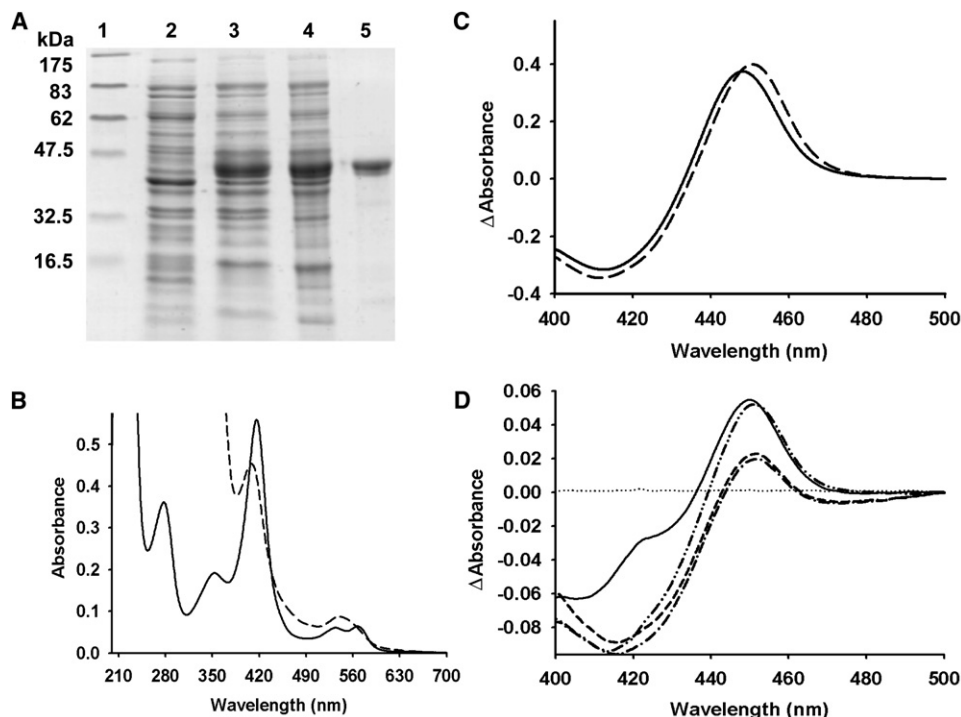


**Figure 3. Characterization of P450s of *So ce56***

(A) SDS-PAGE of expression and purification of CYP109D1. CYP109D1 samples were taken at different stages of expression and purification. Lane 1, prestained protein marker (BioLab). Lane 2, cell lysate before induction with IPTG. Lane 3, cell lysate after 36 hr of expression. Lane 4, cell free supernatant after sonication. Lane 5, purified CYP109D1.

(B) Typical UV-visible spectra of purified CYP266A1 in the absence of substrate. The oxidized (solid line) and dithionite reduced (long dashed) form of CYP266A1 illustrates the typical nature of P450s. The base line was recorded between 200 nm to 700 nm. The UV-visible spectra of P450s (5  $\mu$ M) were recorded in 50 mM potassium phosphate buffer (pH 7.5). The enzymes were reduced by addition of a few grains of sodium dithionite and spectra were measured under the same conditions as mentioned before (see also Table S1).

(C) Spectroscopic characterization of *Sorangium cellulosum* So ce56 P450s. The typical CO-difference spectra of CYP266A1 (solid line) and CYP109D1 (long dashed), showing peak maxima at 448 nm and 450 nm, respectively are shown. The solution of P450 enzyme (5  $\mu$ M) in 50 mM potassium phosphate buffer (pH 7.5) was reduced with a few grains of sodium dithionite to reduce the heme iron. The sample was split into two cuvettes and a base line was recorded between 400 and 500 nm. The sample cuvette was bubbled gently with CO for 30 s and a spectrum was recorded. The concentration of the P450s was estimated by CO-difference spectra assuming  $\Delta\epsilon_{(450-490)} = 91 \text{ mM}^{-1}\text{cm}^{-1}$  (see also Table S1).

(D) Determination of autologous and heterologous electron transfer partners. The dithionite reduced CO-difference spectrum (solid line) of CYP109D1 was compared with the NADPH reduced AdR-Adx (dashed with double dots), Fdx2-FdR\_B (dashed with single dot) and Fdx8-FdR\_B (long dashed) CO-complexed spectrum in the absence of fatty acids. The base line is shown as dotted line. The NADPH (1 mM) reduced CO-difference spectra were recorded in a 1 ml mixture of CYP109D1/Fdx2/Fdx8/Adx/FdR\_B/AdR of 1:10:3 (200 pmol:2 nmol:600 pmol) in 10 mM potassium phosphate buffer, pH 7.5 containing 20% glycerol (see also Table S2).

### Expression, Purification, and Spectrophotometric Characterization of Fatty Acid Hydroxylating Recombinant Cytochromes P450

The potential fatty acid hydroxylating P450 genes were cloned in pCWori<sup>+</sup> vectors and were heterologously expressed in *Escherichia coli* BL21 or JM109. These P450s were expressed in a soluble form and were purified (Figure 3A). The yield of the purified CYP109D1, CYP264A1, and CYP266A1 was 205, 440, and 1400 nmol L<sup>-1</sup>, respectively.

Ultraviolet (UV)-visible absorption spectra of the three fatty acid hydroxylase P450s were recorded for the oxidized and reduced form. The oxidized forms of the purified P450s showed typical spectral properties for the members of the P450 enzyme class with the major Soret ( $\gamma$ ) band located between 415–417 nm, the smaller  $\beta$  band at 535–540 nm, and the  $\alpha$  band at 566–570 nm (Figure 3B; Table S1). The sodium dithionite

reduced spectra of the P450s showed diminished absorption maxima in the Soret region. These typical features are also observed in other well characterized P450s like CYP101 (P450cam) and CYP102A1 (P450-BM3) (Sligar, 1976; Miles et al., 1992). The typical peak maximum in CO-difference spectra was at either 450 nm or 448 nm (Figure 3C; Table S1). The Soret shift from  $\sim$ 418 nm (for ferric low-spin enzyme) to  $\sim$ 450 nm (for the Fe<sup>II</sup>-CO complex) is a “hallmark” of the P450s and an indicative of native (thiolate i.e., cysteinate-coordinated) Fe<sup>II</sup>-CO complexes of the P450s (Estabrook, 2003).

### Identification of Electron Transfer Partners

Because cytochromes P450 are external monooxygenases, they, in general, need an electron transfer system to allow oxygen activation and substrate conversion (Bernhardt, 1996).

This necessity can be fulfilled either by autologous (natural) or heterologous electron donor partners.

It is known that bacterial P450s can cooperate with a variety of heterologous electron transfer proteins (Hannemann et al., 2007). Considering this, the commercially available spinach ferredoxin and ferredoxin reductase were at first used in these studies. However, none of the tested P450s (CYP109D1, CYP264A1, and CYP266A1) was able to accept electrons from the spinach system. As a second combination, bovine adrenodoxin (Adx) and adrenodoxin reductase (AdR) were tested. The typical CO-difference peak of reduced CYP109D1 (~91%) and CYP264A1 (~100%) was obtained using NADPH (Figure 3D; Table S2). These results showed that the heterologous redox partners, Adx and AdR, were efficient enough to transfer, at least, the first electron to CYP109D1 and CYP264A1. This observation supports our previous findings where Adx and AdR could deliver electrons to CYP106A2 from *B. megaterium* for steroid hydroxylation (Hannemann et al., 2006; Virus and Bernhardt, 2008). However, when using CYP266A1, no reduction of the P450 could be detected with the heterologous redox partners.

After being able to transfer electrons from a heterologous redox system to CYP109D1 and CYP264A1 (but not CYP266A1), the very recently identified autologous redox systems of *S. cellulosum* So ce56 (Ewen et al., 2009) were also used to study their efficiency with the P450s. It was found that the three P450s—CYP109D1 (~35%), CYP264A1 (~69%), and CYP266A1 (~80%)—were able to get electrons from both the combinations Fdx2-FdR\_B and Fdx8-FdR\_B although with less efficiency than from the heterologous system (Figure 3D; Table S2).

### Characterization of Substrate Binding

Binding of the substrates to the P450s normally induces a shift in the equilibrium of the heme iron spin toward the high spin form leading to changes in the Soret region of the absorption spectrum (Noble et al., 1999). Saturated fatty acids (lauric acid, myristic acid, and palmitic acid) were selected for binding studies with the myxobacterial P450s. All the tested fatty acids showed perturbation of the heme spectrum of CYP109D1 and CYP266A1 (Figures S2 and S3) with a type I shift of the Soret band from ~418 nm toward ~390 nm, typical for the high spin form of the heme iron. Such a spin shift was not observed for CYP264A1 with any of the tested fatty acids. The binding of the saturated fatty acids with CYP109D1 was much tighter than with CYP266A1. The apparent dissociation constant ( $K_D$ ) of CYP109D1 for the substrates, lauric acid, myristic acid, and palmitic acid was found to be 9, 44, and 20 times, respectively, lesser than with CYP266A1 (Table 2; Figures S2 and S3).

### Functional Characterization of CYP109D1

Because only CYP109D1 displayed a high-spin shift on substrate addition and could also be reduced by the autologous as well as the heterologous redox systems, CYP109D1 was used for a further detailed enzymatic characterization. CYP264A1 was reduced but did not show a type I binding spectrum with any of the tested substrates. Because substrate conversion can also occur in cases where no high spin-shift has been observed (Simgen et al., 2000), we checked, whether CYP264A1 is able

**Table 2. Analysis of the Properties of Fatty Acid Hydroxylating P450s of *So ce56***

Substrate	Lauric Acid	Myristic Acid	Palmitic Acid
Binding constant [ $K_D$ , $\mu\text{M}$ ] <sup>a</sup>			
CYP109D1	0.28 ± 0.06	0.21 ± 0.02	0.47 ± 0.05
CYP264A1	— <sup>b</sup>	—	—
CYP266A1 <sup>a</sup>	2.55 ± 0.25	9.27 ± 1.07	9.73 ± 1.43
Hydroxylation by CYP109D1			
Regioselectivity <sup>f</sup>	$\omega$ -1 to $\omega$ -3	$\omega$ -1 to $\omega$ -5	$\omega$ -5 and $\omega$ -6
Catalytic activity <sup>c</sup>			
Autologous redox partners			
Fdx2-FdR_B	0.025 ± 0.002	0.031 ± 0.001	0.038 ± 0.002
Fdx8-FdR_B	0.040 ± 0.002	0.072 ± 0.001	0.051 ± 0.001
Heterologous redox partners			
Adx-AdR	0.130 ± 0.006	ND	ND
Kinetic parameter <sup>d</sup>			
$K_m$	199.12 ± 49.83	ND	ND
$V_{max}$	0.22 ± 0.03		

ND: not determined. The binding constant of CYP109D1 and CYP266A1 with lauric acid, myristic acid and palmitic acid is compared (see also Figures S2 and S3). The analysis of the properties of CYP109D1-catalyzed regioselective hydroxylation of the saturated fatty acids with autologous and heterologous redox partners is shown (see also Figures S4 and S5).

<sup>a</sup> Although binding occurs, it was not able to convert any of the tested fatty acids.

<sup>b</sup> No binding with the tested substrates.

<sup>c</sup> Nanomoles total product per nmol CYP109D1 per min.

<sup>d</sup> Only studied with heterologous redox partners.

<sup>e</sup> See also Figures S2 and S3.

<sup>f</sup> See also Figures S4 and S5.

to convert the three fatty acids. Unfortunately, no hydroxylated products could be detected (data not shown). Though CYP266A1 bound the substrates and could be reduced with the autologous redox systems, the product was not observed. The in vitro conversions of the saturated fatty acids catalyzed by CYP109D1 were performed using both the autologous (Fdx2-FdR\_B and Fdx8-FdR\_B) redox partners and were measured using gas chromatography-mass spectrometry (GC-MS) after trimethylsilyl (TMS) derivatization. CYP109D1 activity could be reconstituted with the autologous redox partners to produce subterminal hydroxylated products of lauric acid, myristic acid, and palmitic acid. Lauric acid was converted into three hydroxylated products, peaks I, II, and III, at the retention time (RT) of 9.33, 9.76, and 10.05 min, respectively (Figure 4A), where the mass spectra showed the characteristic fragment ions related to 9-, 10-, and 11-hydroxy-dodecanoatrimethylsilyl ether derivatives, respectively, (Figures 4B–4D) and related to  $\omega$ -3,  $\omega$ -2, and  $\omega$ -1 hydroxylated product, respectively. The reconstituted system was also able to convert myristic acid into five hydroxylated products, peaks I (RT 12.51 min), II (RT 12.66 min), III (RT 12.93 min), IV (RT 13.39 min), and V (RT 13.64 min) (Figure S4). The characteristic mass spectra of peaks I–V were related to 9-, 10-, 11-, 12- and 13-hydroxy-tetradecanoatrimethylsilylether derivatives, respectively. This indicates that the

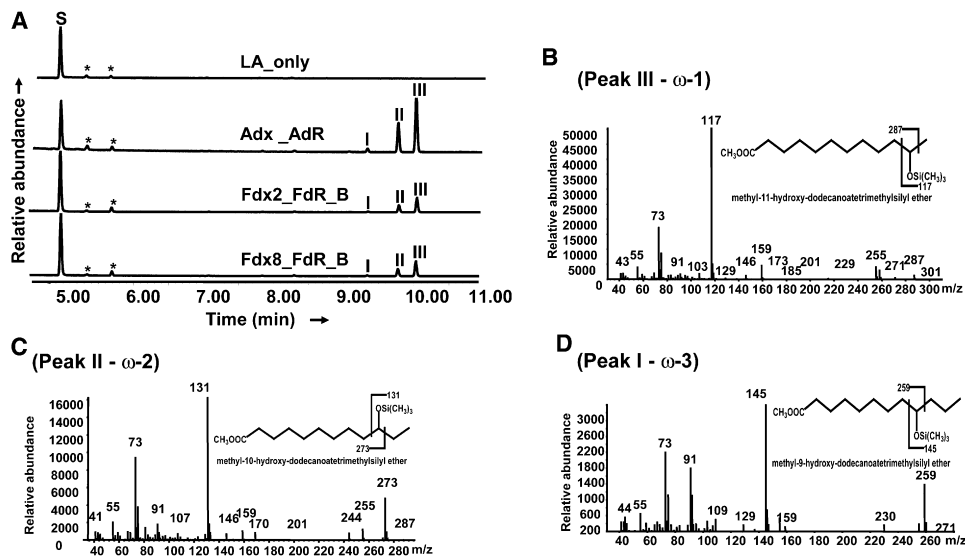


**Figure 4. Analysis of the Hydroxylation of Lauric Acid by CYP109D1**

(A) GC chromatograms of lauric acid conversion. CYP109D1 dependent hydroxylation supported by both the autologous (Fdx2-FdR\_B and Fdx8-FdR\_B) and heterologous (Adx-AdR) redox partners are compared with the negative control, lauric acid only (LA\_only). The GC chromatograms of lauric acid conversion show three hydroxylated product peaks, I, II, and III, at retention times of 9.33, 9.76, and 10.05 min, respectively. In the figure, "S" represents the substrate peak. \*Denotes impurities during GC conversion.

(B–D) Gas chromatography-mass spectrometry (GC-MS) analysis of hydroxylation positions in lauric acid. MSTFA [N-Methyl-N-(trimethylsilyl) trifluoroacetamide] derivatized products of lauric acid were analyzed through GC-MS. The MS fragmentation pattern of peak III (B), peak II (C), and I (D) are shown and compared to archived MS spectra of trimethylsilyl-(TMS) methyl-hydroxy fatty acids (<http://www.lipidlibrary.co.uk>). Peak I, II, and III were identified as methyl-9-hydroxy- (m/z 145 and 259); methyl-10-hydroxy- (m/z 131 and 273), and methyl-11-dodecanoatrimethylsilyl ether, indicated by m/z 117 and 287, corresponding to  $\omega$ -3,  $\omega$ -2, and  $\omega$ -1 hydroxylation, respectively. The inset on each MS illustrates the derivatized units.

peaks I, II, III, IV, and V correspond to  $\omega$ -5,  $\omega$ -4,  $\omega$ -3,  $\omega$ -2, and  $\omega$ -1 hydroxylated products, respectively. Moreover, a long chain saturated fatty acid, palmitic acid, was also converted into two hydroxylated products, peaks I (RT 15.86 min) and II (RT 15.96 min), by CYP109D1 (Figure S5) that correspond to 10- and 11-hydroxy-hexadecanoatrimethylsilyl ether derivatives, respectively. This indicates that the peaks I and II correspond to  $\omega$ -6 and  $\omega$ -5 hydroxylated products, respectively. All GC peaks showed mass spectra indicating a single hydroxylation of saturated fatty acids. The difference between the product peaks displayed by a mass shift of  $\pm 14$  of the two characteristic fragment peaks that is consistent with the loss of a  $-\text{CH}_2$ -unit. The obtained mass spectra of the tested fatty acids are consistent with the existing literature of hydroxylated fatty acid TMS ester (Koo et al., 2002; Wood et al., 2001).

The efficiency of total product formation with the reconstituted autologous redox systems was also studied. It was found that the autologous redox partner Fdx8-FdR\_B was more efficient than the redox pair Fdx2-FdR\_B for tested fatty acids (Figure 5A). The rate of lauric acid, myristic acid and palmitic acid conversion by CYP109D1 with the redox pair Fdx8-FdR\_B was almost 1.6, 2.3, and 1.3 times, respectively, higher than with Fdx2-FdR\_B (Table 2).

The activity of CYP109D1 with the heterologous redox partners, Adx and AdR, was also studied for the lauric acid hydroxylation. The in vitro conversion gave the same regioselective  $\omega$ -3,  $\omega$ -2, and  $\omega$ -1 hydroxylated products as those observed with the autologous redox partners (Figure 4A). Interestingly, the efficiency of total product formation with the heterologous redox

partners was  $0.130 \pm 0.006$  nmol total product per nmol CYP109D1 per min, and thus five and three times higher than the product formation using the autologous redox pairs Fdx2-FdR\_B and Fdx8-FdR\_B, respectively (Figure 5B and Table 2).

The analysis of the substrate conversion kinetics was therefore performed using the reconstituted heterologous redox system because it was the most effective one for lauric acid conversion. In the first step, the Adx-dependent reaction under substrate (lauric acid) saturation conditions was studied for CYP109D1. The  $K_m$  value for Adx under saturating conditions of lauric acid by CYP109D1 was  $6.37 \pm 0.56$   $\mu\text{M}$  (Figure 5C). In a second step, the lauric acid dependent kinetics catalyzed by CYP109D1 was analyzed for the total subterminal ( $\omega$ -1,  $\omega$ -2, and  $\omega$ -3) hydroxylated products. For all these studies, a fixed Adx concentration of 10  $\mu\text{M}$  was used. As shown in Figure 5D, the recombinant CYP109D1 efficiently converted the substrate lauric acid with a  $V_{\text{max}}$  of  $0.22 \pm 0.03$  nmol total product per nmol CYP109D1 per min and a  $K_m$  of  $199 \pm 49$   $\mu\text{M}$  ( $R = 0.99$ ).

## DISCUSSION

Myxobacteria attract many researchers because of their pharmaceutical importance (Wenzel and Müller, 2009, 2007) and complex physiology (Whilworth, 2007; Kaiser 2003; Bode et al., 2006; Curtis et al., 2006). Taking the multiple functions during the life cycle of myxobacteria into account, it can be speculated that the members of the cytochrome P450 family that are distributed all over the genome of Soce56 might be of importance in endogenous physiological processes as well as in secondary

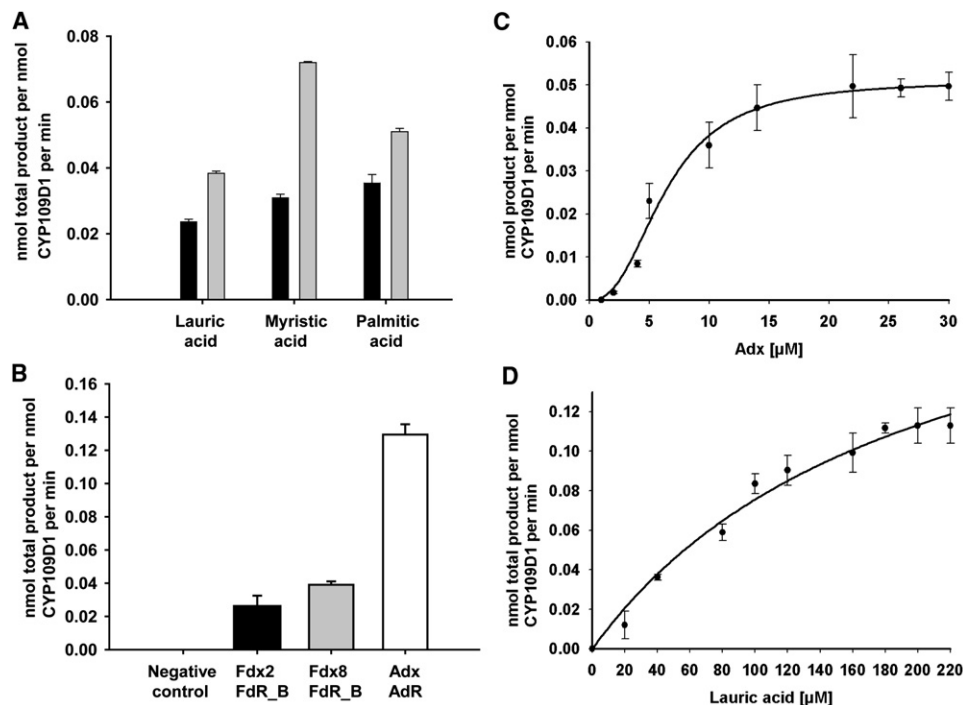


**Figure 5. Enzyme activity of CYP109D1**

(A) Comparison of the CYP109D1-catalyzed product formation rate using different combinations of autologous redox partners. The overall subterminal hydroxylated products of lauric acid, myristic acid and palmitic acid catalyzed by CYP109D1 with the reconstituted autologous, Fdx2-FdR<sub>B</sub> (black column) and Fdx8-FdR<sub>B</sub> (gray column) redox partners are shown. The values represent the mean of three reactions (see also Table 2; Figures S4 and S5).

(B) Comparison of CYP105D1 catalyzed lauric acid hydroxylation by using autologous and heterologous redox partners. The overall subterminal hydroxylated products of lauric acid with the reconstituted system Fdx2-FdR<sub>B</sub> (black column), Fdx8-FdR<sub>B</sub> (gray column), and Adx-AdR (white column) are shown.

(C and D) Kinetic studies of lauric acid hydroxylation catalyzed by CYP109D1 after reconstitution with the heterologous redox partners, Adx and AdR. CYP109D1 catalyzed substrate dependent conversion assays were performed using the reconstituted electron transfer chain consisting of bovine Adx and AdR. Lauric acid hydroxylation was analyzed by GC-MS as described in Experimental Procedures. The bar on each point represents the standard deviation calculated from three individual experiments. In (C), the sigmoidal fit of the Adx-dependent CYP109D1 catalyzed product formation reactions under substrate saturation condition is shown. Several concentrations of Adx (0–30  $\mu$ M) with a fixed concentration of lauric acid (300  $\mu$ M) were used. In (D), CYP109D1-dependent conversion of lauric acid to subterminal hydroxylated products is shown. Different concentrations of lauric acid (20–220  $\mu$ M) were used. The ratio of CYP109D1/Adx/AdR was 1:10:1.

metabolite formation. As members of the cytochrome P450 superfamily are able to catalyze fatty acid hydroxylation (Green et al., 2001; Chun et al., 2007), these enzymes could be of vital importance for the life cycle of myxobacteria. It is conceivable that the resulting hydroxylated products of the P450 dependent fatty acid conversion could successively be converted into related alcohols and carboxylic acids, which could play an important role during normal homeostasis or during other biosynthetic processes. It has been shown that the  $\omega$ -hydroxylation of fatty acids and their successive conversion to primary alcohols and dicarboxylic acids is a significant pathway in the fatty acid metabolism during starvation in higher species (Lu et al., 1969; Dobritsa et al., 2009). Moreover, it has also been shown that the fatty acid dependent signaling is attenuated by P450 mediated hydroxylations in bacteria (English et al., 1997).

Interestingly, the fatty acid composition of the vegetative cells of the model myxobacterium *Myxococcus xanthus* DK1622 has shown that two fatty acids, iso-15:0 (40.10%) and 16:w1c (17.04%), are predominant along with several 2- and 3-hydroxylated fatty acids (Bode et al., 2009). Moreover, the fatty acids

profile of vegetative cells of *S. cellulosum* So ce56 also showed the presence of saturated and hydroxylated fatty acids (Table S3). The straight chain fatty acids, their hydroxylated products and the derivatives are likely targets for a number of modifications during the complex life cycle required for the gliding motility and cell signaling.

To investigate a possible formation of hydroxylated fatty acids in the myxobacterium So ce56, we have identified and characterized the CYPome of this myxobacterium. Out of 21 cytochromes P450, 10 P450s were found to be potential fatty acid hydroxylases due to similarities to known fatty acid converting P450s (P450Biol and CYP105D5) and three P450s (CYP109D1, CYP264A1, and CYP266A1) were selected for detailed studies. Due to their character as external mono-oxygenases, the biological activity of the P450s cannot be explored without an efficient electron transfer system. Therefore, we investigated potential heterologous and autologous natural redox partners. The heterologous electron donor proteins spinach ferredoxin reductase (FdR) and ferredoxin (Fdx) that are often employed as electron transfer partners in the reconstitution of bacterial P450s systems, did not work with any of the tested P450s

(CYP109D1, CYP264A1, and CYP266A1) of So ce56, whereas Adx-AdR worked except for CYP266A1.

Very recently, we have identified eight ferredoxins and two reductases in the genome of *S. cellulosum* So ce56. However, we could heterologously express and purify only five of the ferredoxins and both the reductases (Ewen et al., 2009). It was shown that two redox chains (Fdx2- FdR\_B and Fdx8- FdR\_B) work well with another cytochrome P450 from So ce56 (CYP260A1) (Ewen et al., 2009). Regarding the second ferredoxin reductase of So ce56 (FdR\_A), it was found that the redox chains consisting of this reductase and Fdx2 or Fdx8 are considerably worse than the ones relying on FdR\_B. The ferredoxins Fdx1, Fdx3 and Fdx5 in combination with any of the reductases were not able to sustain the enzymatic activity (Ewen et al., 2009). Thus, we focused on the two autologous electron transfer chains Fdx2- FdR\_B and Fdx8- FdR\_B that were used during the reconstitution assay for CYP109D1, CYP264A1, and CYP266A1. Surprisingly, CYP266A1 was also not able to convert any of the tested fatty acids, although the autologous redox partners were able to transfer at least the first electron, and a type I spin shift was observed. CYP264A1 was also not able to hydroxylate the tested fatty acids. However, we were able to show that both the autologous (Fdx2-FdR\_B and Fdx8-FdR\_B) and heterologous (Adx-AdR) redox partners transferred electrons to CYP109D1 for the hydroxylation of saturated fatty acid at sub-terminal positions.

In summary, 21 P450s encoding ORFs from the myxobacterium *S. cellulosum* So ce56 were identified and nine novel P450 families were disclosed. A phylogenetic tree and a physical map of P450s of So ce56 were constructed. The molecular cloning, heterologous expression, and the purification of the three fatty acid hydroxylating P450s genes (CYP109D1, CYP264A1, and CYP266A1) were done for detailed characterization. The putative substrates (lauric acid, myristic acid, and palmitic acid) were not able to induce a spin shift with CYP264A1. In contrast, CYP109D1 and CYP266A1 underwent high-spin shifts after binding those fatty acids, with CYP109D1 showing higher affinity. The autologous redox partners (Fdx2-FdR\_B and Fdx8-FdR\_B) were able to transfer electrons to all three P450s. In addition, the heterologous redox partners Adx and AdR also allowed the transfer of electrons to CYP109D1 and CYP264A1. CYP109D1 was able to hydroxylate lauric acid, myristic acid and palmitic acid into sub-terminal position by using the autologous electron transfer systems. Interestingly, the heterologous electron transfer system turned out to be more effective than the two autologous ones during lauric acid conversion and thus, lauric acid dependent kinetic analysis of CYP109D1 was also performed with this system.

## SIGNIFICANCE

**The genome sequence of *Sorangium cellulosum* So ce56 revealed 21 open reading frames for cytochromes P450s. Here, we performed the first and comprehensive bioinformatic analysis of all the P450s. The nomenclature of those P450s, done by Dr. David Nelson (University of Tennessee Health Science Center), revealed nine novel bacterial P450 families. A phylogenetic tree as well as a physical map of the P450s has been deduced from this data. Considering**

**the importance of fatty acids during the complex life cycle of myxobacteria, it was a point of interest to identify potential fatty acid hydroxylating P450s of So ce56. The alignment of the So ce56 CYPome with the well characterized P450s showed 10 potential fatty acid hydroxylating P450s genes. Three of the P450s (CYP109D1, CYP264A1, and CYP266A1) were cloned, heterologously expressed in a soluble form in *Escherichia coli* and showed absorption peaks of the reduced CO-bound protein with maxima at 450 or 448 nm. Although it was not possible to show a functional role for CYP264A1 and CYP266A1 due to the absence of potential substrates or efficient redox partners, CYP109D1 was demonstrated to be a new fatty acid hydroxylase. We have disclosed two autologous electron transfer paths,  $\text{NADPH} \rightarrow \text{FdR}_B \rightarrow \text{Fdx2} \rightarrow \text{CYP109D1}$  and  $\text{NADPH} \rightarrow \text{FdR}_B \rightarrow \text{Fdx8} \rightarrow \text{CYP109D1}$  for the subterminal hydroxylation of saturated fatty acids. The abundance of saturated fatty acids especially palmitic acid in the vegetative cells of the bacterium, and the sub-terminal hydroxylation of palmitic acid as well as lauric acid and myristic acid with autologous redox partners signifies the potential physiological importance of the fatty acid hydroxylating P450s in *S. cellulosum* So ce56. Furthermore, we have disclosed an effective heterologous redox path,  $\text{NADPH} \rightarrow \text{AdR} \rightarrow \text{Adx} \rightarrow \text{CYP109D1}$  for lauric acid conversion. Finally, the kinetics of the CYP109D1-dependent fatty acid hydroxylation were also analyzed.**

## EXPERIMENTAL PROCEDURES

### Bioinformatic Analysis

Cytochrome P450s encoding open reading frames (ORFs) of *S. cellulosum* So ce56 were analyzed in the genomic database based on the heme-binding domain signature, FxxGx(H/R)xCxG as query sequence. The ORFs possessing such motifs were further analyzed for the presence of the highly conserved threonine in the putative I-helix and the conserved EXXR motif in the K-helix (Nelson et al., 1996; Denisov et al., 2005). Amino acid sequences were deduced from the genes by using "Expasy Translation Tool." The P450 families and subfamilies were assigned by Dr. David Nelson (<http://drnelson.utmem.edu/CytochromeP450.html>). Briefly, P450s showing >40% identity were placed in the same family and those exhibiting >55% identity were categorized in the same subfamily. New families were assigned for the P450s showing <40% identity to known proteins from other organisms.

### Phylogenetic Analysis

Translated ORFs of respective P450 genes of So ce56 CYPome were aligned using Clustal W (Thompson et al., 1994) and were analyzed by the Neighbor Joining Algorithm with boot strap values of 1000 times replicating to resample the data and displayed through Tree View (Page, 1996). A physical map of the 13.1 Mb sized genome of So ce56 was prepared manually with the allocated positions of P450s, ferredoxins (Fdx) and ferredoxin reductases (FdR) according to the database in the genome.

### Molecular Cloning of Cytochrome P450 Encoding Genes

The genomic DNA of So ce56 was extracted as described before (Perlova et al., 2006). The expression vectors of the putative fatty acid hydroxylating cytochrome P450s encoding genes (CYP109D1, CYP264A1, and CYP266A1) were prepared in pCWori<sup>+</sup> as described in Supplemental Experimental Procedures 1.

### Heterologous Gene Expression and Purification of His<sub>6</sub>-Cytochrome P450s

*E. coli* strains BL21 and JM109 were used as heterologous hosts for the expression of all the P450s. The fatty acid hydroxylating P450s were

overexpressed and purified as described in Supplemental Experimental Procedures 2.

#### Purification of his-Tagged Ferredoxins Fdx2, Fdx8, Ferredoxin Reductases FdR\_B, Adx, and AdR

The expression and purification of Fdx2, Fdx8 and FdR\_B of *S. cellulosum* So ce56 were done as described before (Ewen et al., 2009). The mammalian truncated adrenodoxin, Adx (4–108) (Uhlmann et al., 1994) and adrenodoxin reductase, AdR, were expressed and purified as described before (Sagara et al., 1993).

#### Spectrophotometric Characterization of P450s

UV-visible spectra for CYP109D1, CYP264A1, and CYP266A1 were recorded at room temperature on a double-beam spectrophotometer (UV-2101PC, SHIMADZU, Kyoto, Japan). The concentration of the P450s was estimated by CO-difference spectra assuming  $\Delta\epsilon_{(450-490)} = 91 \text{ mM}^{-1} \text{ cm}^{-1}$  according to the method of Omura and Sato (Omura and Sato, 1964).

#### Investigation of Electron Transfer Partners

In general, to illustrate the functional role of the P450s, efficient redox partners (either autologous or heterologous), should be available. In this study, both options were carried out. The competency of the electron transfer partners for a particular P450 was determined by recording the NADPH reduced CO-complex peak at 450 nm peak coupled with the different ferredoxins/ferredoxin reductases in the absence of fatty acids as described in Supplemental Experimental Procedures 3.

#### Spin-State Shift and Substrate Dissociation Constant Determination

The spin-state shifts on substrate binding were assayed at room temperature under aerobic condition using an UV-Vis scanning photometer (UV-2101PC, Shimadzu, Japan) equipped with two tandem cuvettes. The dissociation constant ( $K_D$ ) for the P450s (CYP109D1 and CYP266A1) with the substrates (lauric acid, myristic acid, and palmitic acid) was calculated by fitting the peak-to-trough difference against the substrate concentration to a nonlinear tight binding quadratic equation as described in Supplemental Experimental Procedures 4.

#### Enzyme Activity Assay

The purpose of the assay was to demonstrate the ability of the P450s to convert fatty acids, the putative natural substrates, into the hydroxylated products during reconstitution with autologous (Fdx2 or Fdx8 and FdR\_B) or heterologous (Adx and AdR) redox partners.

The *in vitro* assay of lauric acid, myristic acid, and palmitic acid with the reconstituted autologous electron partners was done for CYP109D1, CYP264A1, and CYP266A1. The assays with autologous electron transport partners (Fdx2-FdR\_B or Fdx8-FdR\_B) were performed with a protein ratio of CYP/Fdx2 or Fdx8/FdR\_B of 1:60:3. For this, the reactions were performed in a final volume of 0.5 ml that contained the respective P450 (1  $\mu\text{M}$ ), Fdx2 or Fdx8 (60  $\mu\text{M}$ ), FdR\_B (3  $\mu\text{M}$ ), and substrate (300  $\mu\text{M}$ ) in buffer D. In addition to this, a NADPH regenerating system, consisting of glucose-6-phosphate (5 mM), glucose-6-phosphate dehydrogenase (1 unit), and magnesium chloride (1 mM) was also applied. After preincubation at 30°C on a thermomixture (Eppendorf), the reaction was started by adding NADPH to 500  $\mu\text{M}$  final concentration and the mixture was incubated for 30 min. The reaction was stopped with an equal volume of GC grade diethyl ether. The product was extracted with diethyl ether for three times and the extract was vacuum dried.

The *in vitro* conversion of lauric acid with the reconstituted heterologous electron partners, Adx and AdR, was done for CYP109D1 and CYP264A1. In the first set of experiments, the study of CYP109D1 activity depending on the Adx concentration under substrate (lauric acid) saturation condition was studied. For this, the reactions were performed in a final volume of 0.5 ml. The reaction mixture consisted of CYP109D1 (1  $\mu\text{M}$ ), AdR (1  $\mu\text{M}$ ), Adx (0–30  $\mu\text{M}$ ), and lauric acid (300  $\mu\text{M}$ ) in buffer A. All other components and methods were the same as those mentioned before.  $V_{\text{max}}$  and  $K_m$  values were determined by plotting the substrate conversion velocities versus the corresponding Adx concentrations and subsequently using a sigmoidal fit (SIGMAPLOT software).

In another set of the experiments, increasing concentration of lauric acid (20–220  $\mu\text{M}$ ) but fixed concentrations of CYP109D1 (1  $\mu\text{M}$ ), Adx (10  $\mu\text{M}$ ), and AdR (1  $\mu\text{M}$ ) were used. All other components and methods were as described above.  $V_{\text{max}}$  and  $K_m$  values were determined by plotting the substrate concentration velocities versus the corresponding substrate concentration and subsequently plotting hyperbolic fit (SIGMAPLOT software). The relevant equation is:  $Y = A \cdot X/B + A$  where “Y” represents the substrate concentration velocities, “A” represents the Y maximum, “B” represents the  $K_D$  value, and “X” represents the lauric acid concentration.

#### GC-MS Analysis of In Vitro Products

The evaporated samples were dissolved in a mixture of 500  $\mu\text{l}$  methanol/toluene/sulphuric acid (50:50:2 V/V/V) and overnight incubation was done at 55°C to form fatty acid methyl ester derivatives. Four hundred microliters of an aqueous reagent (0.5 M  $\text{NH}_4\text{HCO}_3$  + 2 M KCl) was added to the samples followed by a short mixing step. Samples were centrifuged at room temperature to achieve a complete phase separation. Seventy-five microliters of the organic phase was transferred to a GC vial and derivatized with 25  $\mu\text{l}$  N-methyl-N-trimethylsilyltrifluoroacetamide (MSTFA) followed by 1 hr incubation at 37°C.

Fatty acid analysis was performed in a gas chromatograph (Agilent 6890N) coupled to an Agilent 5973N electron impact mass selective detector equipped with a nonpolar capillary column (J&W DB-5HT, 30 m  $\times$  0.25 mm  $\times$  0.10  $\mu\text{m}$ ). One microliter of the sample was injected using a 1:10 split mode. The helium flow rate was set to 1 ml/min and inlet and GC-MS transfer line temperatures were held at 275°C. The column oven temperature was initially set to 130°C and held for 2.5 min, then increased to 240°C at a rate of 5°C/min and finally increased to 300°C at a rate of 30°C/min and held for 5 min.

#### SUPPLEMENTAL INFORMATION

Supplemental Information includes Supplemental Experimental Procedures, five figures, and four tables and can be found with this article online at doi:10.1016/j.chembiol.2010.10.010.

#### ACKNOWLEDGMENTS

This work was supported by the fellowship awarded by Deutscher Akademischer Austausch Dienst (DAAD) to Y.K. and N.K., and a grant of the Fonds der Chemischen Industrie to R.B. Research in R.M.'s laboratory was funded by a grant from the Bundesministerium für Bildung und Forschung (BMBF). We thank Prof. Dr. Michael R. Waterman, Vanderbilt University School of Medicine, Nashville, TN, USA, for the gift of expression vector pCWori<sup>+</sup>. We are thankful to Wolfgang Reinle for expression and purification of Adx and AdR. We also express our sincere gratitude to Dr. David Nelson, University of Tennessee Health Science Center, USA for the nomenclature of cytochrome P450 and to Dr. Vlada B. Urlacher, Institute for Technical Biochemistry, University of Stuttgart for worthy suggestions.

Received: April 27, 2010

Revised: September 13, 2010

Accepted: October 8, 2010

Published: December 21, 2010

#### REFERENCES

- Bernhardt, R. (1996). Cytochrome P450: structure, function and generation of reactive oxygen species. *Rev. Physiol. Biochem. Pharmacol.* 127, 137–221.
- Bernhardt, R. (2006). Cytochromes P450 as versatile biocatalysts. *J. Biotechnol.* 124, 128–145.
- Bode, H.B., Dickschat, J.S., Kroppenstedt, R.M., Schulz, S., and Muller, R. (2005). Biosynthesis of iso-fatty acids in myxobacteria: iso-even fatty acids are derived by alpha-oxidation from iso-odd fatty acids. *J. Am. Chem. Soc.* 127, 532–533.
- Bode, H.B., Ring, M.W., Kaiser, D., David, A.C., Kroppenstedt, R.M., and Schwar, G. (2006). Straight-chain fatty acids are dispensable in the

- myxobacterium *Myxococcus xanthus* for vegetative growth and fruiting body formation. *J. Bacteriol.* **188**, 5632–5634.
- Bode, H.B., Ring, M.W., Schwäre, G., Altmeyer, O.M., Kegler, C., Jose, R.I., Singer, M., and Müller, R. (2009). Identification of additional players in the alternative biosynthesis pathway to isovaleryl-CoA in the myxobacterium *Myxococcus xanthus*. *ChemBioChem* **10**, 128–140.
- Buntin, K., Rachid, S., Scharfe, M., Blöcker, H., Weissman, J.K., and Müller, R. (2008). Production of the antifungal isochromanone ajdazols A and B in *Chondromyces crocatus* Cm c5: biosynthetic machinery and cytochrome P450 modifications. *Angew. Chem. Int. Ed. Engl.* **47**, 4595–4599.
- Chun, Y.J., Shimada, T., Sanchez-Ponce, R., Martin, M.V., Lei, L., Zhao, B., Kelly, S.L., Waterman, M.R., Lamb, D.C., and Guengerich, F.P. (2007). Electron transport pathway for a *Streptomyces* cytochrome P450: cytochrome P450 105D5-catalyzed fatty acid hydroxylation in *Streptomyces coelicolor* A3 (2). *J. Biol. Chem.* **282**, 17486–17500.
- Curtis, P.D., Geyer, R., White, D.C., and Shmickets, L.J. (2006). Novel lipids in *Myxococcus xanthus* and their role in chemotaxis. *Environ. Microbiol.* **8**, 1935–1949.
- Davis, S.C., Sui, Z., Peterson, J.A., and Ortiz de Montellano, P.R. (1996). Oxidation of omega-oxo fatty acids by cytochrome P450BM-3 (CYP102). *Arch. Biochem. Biophys.* **328**, 35–42.
- Dawson, J.H., Holm, R.H., Trudell, J.R., Barth, G., Linder, R.E., Bunnenberg, E., Djerassi, C., and Tang, S.C. (1976). Oxidized cytochrome P-450. Magnetic circular dichroism evidence for thiolate ligation in the substrate-bound form. Implications for the catalytic mechanism. *J. Am. Chem. Soc.* **98**, 3707–3708.
- Denisov, I.G., Makris, T.M., Sligar, S.G., and Schlichting, I. (2005). Structure and chemistry of cytochrome P450. *Chem. Rev.* **105**, 2253–2278.
- Dobritsa, A.A., Shrestha, J., Morant, M., Pinot, F., Matsuno, M., Swanson, R., Möller, B.L., and Preuss, D. (2009). CYP704B1 is a long-chain fatty acid (omega)-hydroxylase essential for sporopollenin synthesis in pollen of arabis. *Plant Physiol.* **151**, 574–589.
- English, N., Palmer, C.N.A., Alworth, W.L., Kang, L., Hughes, V., and Wolf, C.R. (1997). Fatty acid signals in *Bacillus megaterium* are attenuated by cytochrome P-450-mediated hydroxylation. *Biochem. J.* **327**, 363–368.
- Estabrook, R.W. (2003). A passion for P450s (remembrances of the early history of research on cytochrome P450). *Drug Metab. Dispos.* **31**, 1461–1473.
- Ewen, K.M., Hannemann, F., Khatri, Y., Perlova, O., Kappl, R., Krug, D., Hüttermann, J., Müller, R., and Bernhardt, R. (2009). Genome mining in *Sorangium Cellulosum* So ce56: identification and characterization of the homologous electron transfer proteins of a myxobacterial cytochrome P450. *J. Biol. Chem.* **284**, 28590–28598.
- Gerth, K., Pradella, S., Perlova, O., Beyer, S., and Müller, R. (2003). Myxobacteria: proficient producers of novel natural products with various biological activities—past and future biotechnological aspects with the focus on the genus *Sorangium*. *J. Biotechnol.* **106**, 233–253.
- Girhard, M., Klaus, T., Khatri, Y., Bernhardt, R., and Urlacher, V.B. (2010). Characterization of the versatile monooxygenase CYP109B1 from *Bacillus subtilis*. *Appl. Microbiol. Biotechnol.* **87**, 595–607.
- Girhard, M., Schuster, S., Dietrich, M., Dürre, P., and Urlacher, V.B. (2007). Cytochrome P450 monooxygenase from *Clostridium acetobutylicum*: a new alpha-fatty acid hydroxylase. *Biochem. Biophys. Res. Commun.* **362**, 114–119.
- Graziani, E.I., Cane, D.E., Betlach, M.C., Kealey, J.T., and McDaniel, R. (1998). Macrolide biosynthesis: A single cytochrome P450, PicK, is responsible for the hydroxylations that generate methymycin, neomethymycin, and picromycin in *Streptomyces venezuelae*. *Bioorg. Med. Chem. Lett.* **8**, 3117–3120.
- Green, A.J., Rivers, S.L., Cheesman, M., Reid, G.A., Quaroni, L.G., Macdonald, I.D., Chapman, S.K., and Munro, A.W. (2001). Expression, purification and characterization of cytochrome P450 Biol: a novel P450 involved in biotin synthesis in *Bacillus subtilis*. *J. Biol. Inorg. Chem.* **6**, 523–533.
- Gustafsson, M.C.U., Roitel, O., Marshall, K.R., Noble, M.A., Chapman, S.K., Pessegueiro, A., Fulco, A.J., Cheesman, M.R., von Wachenfeldt, C., and Munro, A.W. (2004). Expression, purification, and characterization of *Bacillus subtilis* cytochromes P450 CYP102A2 and CYP102A3: flavocytochrome homologues of P450 BM3 from *Bacillus megaterium*. *Biochemistry* **43**, 5474–5487.
- Hannemann, F., Bichet, A., Ewen, K.M., and Bernhardt, R. (2007). Cytochrome P450 systems—biological variations of electron transport chains. *Biochim. Biophys. Acta* **1770**, 330–344.
- Hannemann, F., Virus, C., and Bernhardt, R. (2006). Design of an *Escherichia coli* system for whole cell mediated steroid synthesis and molecular evolution of steroid hydroxylases. *J. Biotechnol.* **124**, 172–181.
- Hasemann, C.A., Kurumbail, R.G., Boddupalli, S.S., Peterson, J.A., and Deisenhofer, J. (1995). Structure and function of cytochromes P450: a comparative analysis of three crystal structures. *Structure* **3**, 41–62.
- Johnston, J.B., Kells, P.M., Podust, L.M., and Ortiz de Montellano, P.R. (2009). Biochemical and structural characterization of CYP124: a methyl-branched lipid omega-hydroxylase from *Mycobacterium tuberculosis*. *Proc. Natl. Acad. Sci. USA* **106**, 20687–20692.
- Kaiser, D. (2003). Coupling cell movement to multicellular development in myxobacteria. *Nat. Rev. Microbiol.* **1**, 45–54.
- Kaneda, T. (1991). Iso- and anteiso-fatty acids in bacteria: biosynthesis, function and taxonomic significance. *Microbiol. Rev.* **55**, 288–302.
- Kitazume, T., Tanaka, A., Takaya, N., Nakamura, A., Matsuyama, S., Suzuki, T., and Shoun, H. (2002). Kinetic analysis of hydroxylation of saturated fatty acids by recombinant P450foxy produced by an *Escherichia coli* expression system. *Eur. J. Biochem.* **269**, 2075–2082.
- Koo, L.S., Immoos, C.E., Cohen, M.S., Farmer, P.J., and Ortiz de Montellano, P.R. (2002). Enhanced electron transfer and lauric acid hydroxylation by site-directed mutagenesis of CYP119. *J. Am. Chem. Soc.* **124**, 5684–5691.
- Lamb, D.C., Ikeda, H., Nelson, D.R., Ishikawa, J., Skaug, T., Jackson, C., Omura, S., Waterman, M.R., and Kelly, S.L. (2003). Cytochrome P450 complement (CYPome) of the avermectin-producer *Streptomyces avermitilis* and comparison to that of *Streptomyces coelicolor* A3(2). *Biochem. Biophys. Res. Commun.* **307**, 610–619.
- Lu, A.Y.H., Junk, K.W., and Coon, M.J. (1969). Reconstituted liver microsomal enzyme system that hydroxylates drugs, other foreign compounds, and endogenous substrates. *J. Biol. Chem.* **244**, 3714–3721.
- Martinis, S.A., Atkins, W.M., Stayton, P.S., and Sligar, S. (1989). A conserved residue of cytochrome P-450 is involved in heme-oxygen stability and activation. *J. Am. Chem. Soc.* **111**, 9252–9253.
- Miles, J.S., Munro, A.W., Rospendowski, B.N., Smith, W.E., McKnight, J., and Thomson, A.J. (1992). Domains of the catalytically self-sufficient cytochrome P-450 BM-3. Genetic construction, overexpression, purification and spectroscopic characterization. *Biochem. J.* **288**, 503–509.
- Mulzer, H.J. (2008). *The Epothilones—An Outstanding Family of Anti-Tumor Agents: From Soil to the Clinic* (Austria: Springer-Verlag).
- Nelson, D.R., Koymans, L., Kamataki, T., Stegeman, J.J., Feyereisen, R., Waxman, D.J., Waterman, M.R., Gotoh, O., Coon, M.J., Estabrook, R.W., et al. (1996). P450 superfamily: update on new sequences, gene mapping, accession numbers and nomenclature. *Pharmacogenetics* **6**, 1–42.
- Noble, M.A., Miles, C.S., Chapman, S.K., Lysek, D.A., MacKay, A.C., Reid, G.A., Hanzlik, R.P., and Munro, A.W. (1999). Roles of key active-site residues in flavocytochrome P450 BM3. *Biochem. J.* **339**, 371–379.
- Omura, T., and Sato, R. (1964). The carbon monoxide-binding pigment of liver microsomes. I. Evidence for its hemoprotein nature. *J. Biol. Chem.* **239**, 2370–2378.
- Ost, T.W., Munro, A.W., Mowat, C.G., Taylor, P.R., Pessegueiro, A., Fulco, A.J., Cho, A.K., Cheesman, M.A., Walkinshaw, M.D., and Chapman, S.K. (2001). Structural and spectroscopic analysis of the F393H mutant of flavocytochrome P450 BM3. *Biochemistry* **40**, 13430–13438.
- Page, R.D.M. (1996). Tree View: An application to display phylogenetic trees on personal computers. *Comput. Appl. Biosci.* **12**, 357–358.
- Perlova, O., Gerth, K., Kaiser, O., Hans, A., and Müller, R. (2006). Identification and analysis of the chivosazol biosynthetic gene cluster from the myxobacterial model strain *Sorangium cellulosum* So ce56. *J. Biotechnol.* **121**, 174–191.

- Presnell, S.R., and Cohen, F.E. (1989). Topological distribution of four-alpha-helix bundles. *Proc. Natl. Acad. Sci. USA* 86, 6592–6596.
- Ring, M.W., Schwär, G., and Bode, H.B. (2009). Biosynthesis of 2-hydroxy and iso-even fatty acids is connected to sphingolipid formation in myxobacteria. *ChemBioChem* 10, 2003–2010.
- Sagara, Y., Wada, A., Takata, Y., Waterman, M.R., Sekimizu, K., and Horiuchi, T. (1993). Direct expression of adrenodoxin reductase in *Escherichia coli* and the functional characterization. *Biol. Pharm. Bull.* 16, 627–630.
- Schneiker, S., Perlova, O., Kaiser, O., Gerth, K., Alici, A., Altmeyer, M.O., Bartels, D., Bekel, T., Beyer, S., Bode, E., et al. (2007). Complete genome sequence of the myxobacterium *Sorangium cellulosum*. *Nat. Biotechnol.* 25, 1281–1289.
- Shirane, N., Sui, Z., Peterson, J.A., and Ortiz de Montellano, P.R. (1993). Cytochrome P450BM-3 (CYP102): regioselectivity of oxidation of omega-unsaturated fatty acids and mechanism-based inactivation. *Biochemistry* 32, 13732–13741.
- Simgen, B., Contzen, J., Schwarzer, R., Bernhardt, R., and Jung, C. (2000). Substrate binding to 15beta-hydroxylase (CYP106A2) probed by FT infrared spectroscopic studies of the iron ligand CO stretch vibration. *Biochem. Biophys. Res. Commun.* 269, 737–742.
- Sligar, S.G. (1976). Coupling of spin, substrate, and redox equilibria in cytochrome P450. *Biochemistry* 15, 5399–5406.
- Thompson, J.D., Higgins, D.G., and Gibson, T.J. (1994). CLUSTAL W: improving the sensitivity of progressive multiple sequence alignment through sequence weighting, position-specific gap penalties and weight matrix choice. *Nucleic Acids Res.* 22, 4673–4680.
- Torres, S., Fjetland, C., and Lammers, P. (2005). Alkane-induced expression, substrate binding profile, and immunolocalization of a cytochrome P450 encoded on the *nifD* excision element of *Anabaena* 7120. *BMC Microbiol.* 5, 16.
- Tully, R.E., Vanberkum, P., Lovins, K.W., and Keister, D.L. (1998). Identification and sequencing of a cytochrome-P450 gene-cluster from *Bradyrhizobium japonicum*. *Biochim. Biophys. Acta* 1398, 243–255.
- Uhlmann, H., Kraft, R., and Bernhardt, R. (1994). C-terminal region of adrenodoxin affects its structural integrity and determines differences in its electron transfer function to cytochrome P-450. *J. Biol. Chem.* 269, 22557–22564.
- Vidakovic, M., Sligar, S.G., Li, H., and Poulos, T.L. (1998). Understanding the role of the essential Asp251 in cytochrome p450cam using site-directed mutagenesis, crystallography, and kinetic solvent isotope effect. *Biochemistry* 37, 9211–9219.
- Virus, C., and Bernhardt, R. (2008). Molecular evolution of a steroid hydroxylating cytochrome P450 using a versatile steroid detection system for screening. *Lipids* 43, 1133–1141.
- Ware, J.C., and Dworkin, M. (1973). Fatty acids of *Myxococcus xanthus*. *J. Bacteriol.* 115, 253–261.
- Wenzel, S.C., and Müller, R. (2007). Myxobacterial natural product assembly lines: fascinating examples of curious biochemistry. *Nat. Prod. Rep.* 24, 1211–1224.
- Wenzel, C.S., and Müller, R. (2009). Myxobacteria—‘microbial factories’ for the production of bioactive secondary metabolites. *Mol. Biosyst.* 5, 567–574.
- Whilworth, D. (2007). *Myxobacteria: Multicellularity and Differentiation* (Chicago: ASM Press).
- Wood, K.V., Bonham, C.C., and Jenks, M.A. (2001). The effect of water on the ion trap analysis of trimethylsilyl derivatives of long-chain fatty acids and alcohols. *Rapid Commun. Mass Spectrom.* 15, 873–877.
- Zhao, B., Lin, X., Lei, L., Lamb, D.C., Kelly, S.L., Waterman, M.R., and Cane, D.E. (2008). Biosynthesis of the sesquiterpene antibiotic albaflavenone in *Streptomyces coelicolor* A3(2). *J. Biol. Chem.* 283, 8183–8189.